JOURNAL OF MATERIALS SCIENCE, 31 (1996) 423–430

Preparation and non-linear optical properties of CdS quantum dots in Na_2O–B_2O_3–SiO_2 glasses by the sol–gel technique

T. TAKADA* J. D. MACKENZIE
Department of Materials Science and Engineering, University of California, Los Angeles, CA 90024-1594, USA

M. YAMANE
Department of Inorganic Materials, Tokyo Institute of Technology, Tokyo 152, Japan

K. KANG, N. PEYGHAMBARIAN
Optical Sciences Center, University of Arizona, Tucson, AZ 85721, USA

R. J. REEVES, E. T. KNOBBE, R. C. POWELL
Department of Chemistry, Oklahoma State University, Stillwater, OK 74078-0447, USA

Non-linear optical properties of CdS quantum dots embedded in the sol–gel derived Na_2O–B_2O_3–SiO_2 glass matrix have been studied using nanosecond degenerate four-wave mixing (DFWM), pump-probe experiments, and time-resolved subpicosecond DFWM measurements. The concentration of CdS microcrystallites was varied from 1.4 to 10.2 wt% while the particle size was controlled to be in the range of 3–6 nm in diameter so that the confinement effects can be realized. The third-order susceptibility, $\chi^{(3)}$, was determined to be of the order of 10^{-7}–10^{-6} e.s.u. near the resonant wavelength between 450 and 470 nm by the nanosecond DFWM and pump-probe experiments, and of the order of 10^{-11}–10^{-10} e.s.u. at the off-resonant wavelength, 580 nm, by a time-resolved DFWM measurement with 400 fs laser pulse. The decay time changed from 0.5 to 50 picoseconds as a function of the size, size distribution and number density of CdS microcrystallites in the glasses. Photodarkening reduced the optical non-linearity of the melt-quenched samples by a factor of ≈ 20, while it had no appreciable effect on that of the sol–gel derived samples.

1. Introduction

Three-dimensional quantum-confinement effects in semiconductor microcrystallites can result in novel optical properties, making these new materials attractive for applications in optoelectronic devices, such as lasers, optical data storage and high speed optical communication [1, 2].

In general, crystal systems have more profound non-linear properties than glassy materials. However, glasses have competitive advantages in comparison to crystals, such as mechanical stability, ease of handling, possible fabrication of large size optics, excellent optical homogeneity, quicker production process and potential lower cost.

CdS_xSe_{1-x} quantum dot doped glasses, which have been used as optical sharp cut-off colour filters, exhibit a very large third-order non-linear susceptibility, $\chi^{(3)}$, of 10^{-8} e.s.u. and rapid on-off switching times of 25 ps [3, 4]. However, experiments which have been conducted in the last few years have revealed a photodarkening effect which is associated with fabrication conditions [5–8]. It is the current consensus among the researchers into optical device fabrication that no glasses commercially available today satisfy the requirements for optical non-linear applications [9]. Therefore, the development of new useful non-linear optical materials with very large optical non-linearity and ultrafast response is crucial for implementation of the technologies of ultrafast laser optics.

By using the sol–gel technique, we have demonstrated that CdS-doped glass with a high $\chi^{(3)}$ of 10^{-7} (e.s.u.) can be prepared with desirable non-linear optical properties for device application [10, 11]. The presence of Na^+ ion in the Na_2O–B_2O_3–SiO_2 glass matrix makes it possible to form a waveguide by the usual ion-exchange method [12, 13].

In the past decades, much of the research has been concentrated on revealing the non-linear mechanisms responsible for the large non-linearity in the CdS_xSe_{1-x} doped filter glasses. The main

* Author to whom all correspondence should be addressed.
Present address: Department of Inorganic Materials, National Institute of Materials and Chemical Research, Tsukuba, Ibaraki 305, Japan.

0022–2461

non-linearity arises from the state filling effect in the quantum confined particles. The optical non-linear surface effects have also been realized which dominate the luminescence from the quantum dots in glasses. The number density of CdS_xSe_{1-x} microcrystallites in the filter glasses is too low (< 1 wt %) and the size distribution (2–16 nm) is too broad for practical applications. The experimental studies have been plagued with either a variation of particle size, or an inability to separate quantum size effects from the changes in the stoichiometry of the precipitated crystals of CdS_xSe_{1-x}, because both the size and ratio of S/Se change with the temperature and time duration of the striking treatment [13].

In this paper, we report work on semiconductor quantum dots embedded in the sol–gel-derived glass matrix containing CdS with the goal of characterizing the optical property changes resulting from variations in the number density (concentration) and crystal size. The non-linear optical properties of the CdS quantum dots (diameter $< 2\,\mathbf{a}_{bohr}$, ~ 5 nm, strong confinement regime) in Na_2O–B_2O_3–SiO_2 glasses are presented. Efforts in sample preparation have been made to decrease the particle size and size distribution, and to increase the concentration of CdS microcrystallites to enhance the optical non-linearity. The average size and size distribution were determined using transmission electron microscopy (TEM). Three types of measurements have been performed: frequency resolved nanosecond DFWM, pump-probe measurements, and time resolved subpicosecond DFWM to evaluate the optical non-linearities near resonance and off-resonance, and to examine the decay process of the excited carriers.

2. Experimental procedure

2.1. Sample preparation and characterization

The samples were prepared by our previously established sol–gel process [10–12]. The process for preparing CdS-doped glasses includes the following steps: preparation of $Cd(OAc)_2$ doped wet gel, precipitation of $Cd(OAc)_2$ microcrystallites in the gel, conversion of $Cd(OAc)_2$ to CdO by heating the gel in O_2, conversion of CdO to CdS by exposing the gel to H_2S, and densification of the CdS-doped gel. The amount and size distribution of the CdS crystallites, which determine the non-linear optical properties of these glasses, depend on the experimental conditions. Fig. 1 illustrates the procedures used to prepare the samples. The gels were first heat-treated to 420 °C for 12 h in O_2 to oxidize $Cd(OAc)_2$, followed by exposure to H_2S gas at 120 °C for 12 h. Finally, the gels were densified at 590 °C in vacuum. The composition of glass matrix was $5Na_2O$–$15B_2O_3$–$80SiO_2$ (mol %).

The amount of CdO in the heat-treated gels, CdS content and the ratio of S/Cd in the glasses were determined using a Jeol JSM-T1200 scanning electron microscope equipped with a Seiko EG&E type SED 8600 energy dispersive X-ray analyser. The CdS crystallites were observed using a Jeol-100CX transmission electron microscope (TEM) operating at 100 kV.

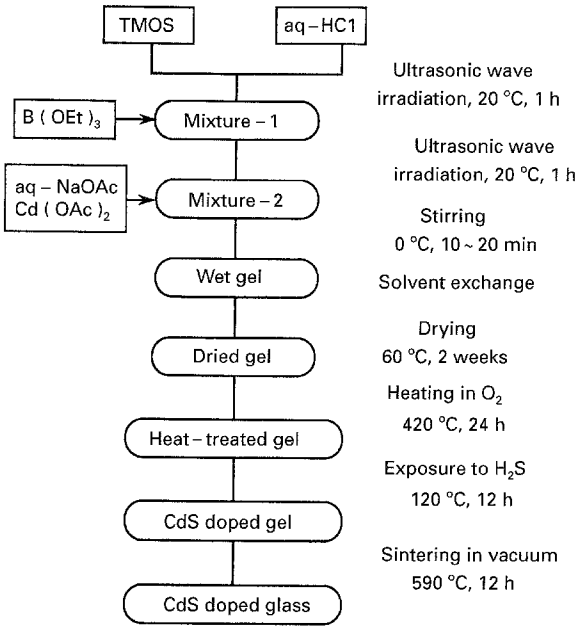

Figure 1 Preparation of CdS doped Na_2O–B_2O_3–SiO_2 glasses by sol–gel process.

High resolution TEM micrographs were obtained using a Jeol JEM 2000 operating at 200 kV.

2.2. Linear and non-linear optical measurement

For all the optical measurements, the glass samples were polished to 15, 20, 19 and 20 μm thick corresponding to the samples A, B, C and D, respectively. All the measurements were made at room temperature. Linear absorption spectra were measured using a Jasco-Uvidec-610C spectrophotometer.

A nanosecond DFWM experiment with two-beam configuration was conducted to determine the $\chi^{(3)}$ value of the samples. The dye laser pulse (7 ns) excited by a N_2 gas laser was tuned from 450 to 470 nm. The pumping intensity was constant at 10 kW cm^{-2}. The experimental DFWM set-up was similar to that of Hiraga and co-workers [14].

The pump-probe measurements were performed to investigate the photoinduced absorption behaviour of CdS microcrystallites in the glasses with 5 ns dye laser pump pulses and white-continuum probe pulses. The energy of the pump pulses was varied from 0.02 to 5 μJ or 5–530 kW cm^{-2}. The wavelength of the pump pulse was 451 nm. The delay time of the probe beams was 3 ns. The experimental set-up has been described elsewhere [15–17].

The time-resolved subpicosecond DFWM experiments were conducted by using a 400 fs laser pulse at a wavelength of 580 nm which was generated from Rhodamine 6G excited by a double YAG. The fluence of laser pulse was 13 mJ cm^{-2}. A variable-delay line was inserted in the backward pump and the probe beam for studying the relaxation process of the transient grating. All beams were polarized in different directions corresponding to the configurations of xyyx, yxyx and xxxx, respectively, for more details, see reference [18].

3. Results and discussion

3.1. Characterization of the sample

Four different samples were used for the non-linear optical experiments. Fig. 2 shows the sol–gel derived CdS doped Na_2O–B_2O_3–SiO_2 glass samples and the corresponding heat-treated CdO doped gels. All samples were optically transparent. The bright yellow colour of the glass samples suggests the presence of CdS crystallites. Note that the CdO contents in this picture represent the nominal values in the precursor solution. The CdO content in the heat-treated gels was less than these values as shown in Table I.

Table I lists the CdO content in the heat-treated gels, CdS content, the ratio of S/Cd and average diameter of CdS crystallites in these samples. The measured CdO content in the heat-treated gels were much lower than that in the precursor solution of the gels, because approximately 30% of $Cd(OAc)_2$ was lost during the gel preparation [10]. In the final glasses, a portion of the Cd species remains as CdO. Under the same conditions of sulphidation, the S/Cd ratio in the glass samples A to D increased from 0.3 to 0.7 as the CdS content increased from 1.4 to 10.2 wt %. Although the average particle size increased with increasing CdS content, they were all in the size regime of strong quantum confinement (Diameter $< 2\,\mathbf{a}_{bohr}$).

TEM micrographs of the samples are shown in Fig. 3. CdS microcrystallites appear as dark particles with sizes ranging from 2 nm to 7 nm. They are randomly distributed in the glass matrix with a large particle number density. The size distribution profiles of CdS crystallites are shown in Fig. 4. The average particle size was determined to be 2.9, 3.7, 4.1 and 4.6 nm corresponding to the samples A, B, C and D, respectively.

A high resolution TEM micrograph of sample C is shown in Fig. 5. A clear fringe pattern can be observed on most particles in this micrograph, indicating the high crystallinity of the particles. These microcrystallites were identified as CdS crystallites of wurtzite structure from the X-ray diffraction pattern as shown in reference [10].

3.2. Linear and non-linear optical properties

Fig. 6 shows the absorption coefficient spectra of the samples near resonance conditions at wavelengths between 350 and 550 nm. The increased blue shift of absorption edge corresponding to the 1s–1s transition [19, 20] with increasing CdS particle size verified the three-dimensional quantum size confinement effect.

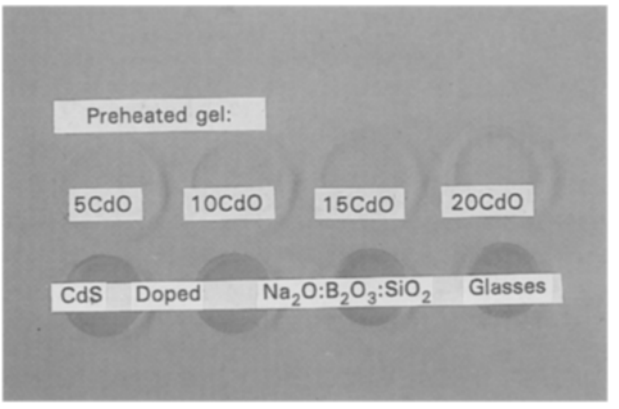

Figure 2 Heat-treated CdO doped gels and CdS doped Na_2O–B_2O_3–SiO_2 glasses.

The threshold energies of these samples (absorption edges) are also found to be linearly proportional to the inverse average square of crystallite radius, consistent with the theoretical predictions described in references [21–23]. It can be seen that the absorption edges of the samples are in the wavelength range of 450–480 nm.

The DFWM measurement gives the absolute value of the third order non-linear coefficient. Fig. 7(a) shows the value of $|\chi^{(3)}|$ determined from the nanosecond DFWM in the vicinity of the resonant wavelengths for the four samples. These results show that for a given sample, $|\chi^{(3)}|$ passes through a maximum at the peak of the 1s–1s transition. The maximum $|\chi^{(3)}|$ value of these samples reached 1.1×10^{-6} e.s.u. at 460 nm. Compared to that of filter glass [3], the value of $|\chi^{(3)}|$ of the sol–gel derived samples has been increased by two orders of magnitude, which indicates that the confinement effect has been enhanced 10–100 times by decreasing the particle size, narrowing the size distribution, and raising the concentration of CdS quantum dots in the glass. For these four samples, the $|\chi^{(3)}|$ value is found to be linearly proportional to concentration of CdS microcrystallites. To exclude the contribution of CdS concentration to $|\chi^{(3)}|$, the value of $|\chi^{(3)}|/\alpha$ is shown in Fig. 7 (b). The $|\chi^{(3)}|/\alpha$ shows very similar profiles as $|\chi^{(3)}|$ versus wavelength, which implies the weak size-dependence of $\chi^{(3)}$ in the size regime of 3–6 nm. Clearly, these results do not support the theoretical model based on quantum size effects that predicts the $1/r^3$ dependence of the non-linearity, where r is the particle radius [24]. Since these results were limited by the tuning ability of the laser wavelength and size broadening of CdS

TABLE I CdO content in the heat-treated gels, CdS content and the size of CdS crystallites in the glass samples

Sample	CdO content		CdS content analysed (wt %)	S/Cd ratio (mol)	Average diameter (nm)
	nominal (mol %)	analysed (mol %)			
A	5	3.9 ± 0.4	1.4 ± 0.3	0.30	2.9
B	10	7.2 ± 0.4	3.8 ± 0.5	0.49	3.7
C	15	10.5 ± 0.4	8.2 ± 0.7	0.68	4.1
D	20	13.6 ± 0.4	10.2 ± 0.7	0.70	4.6

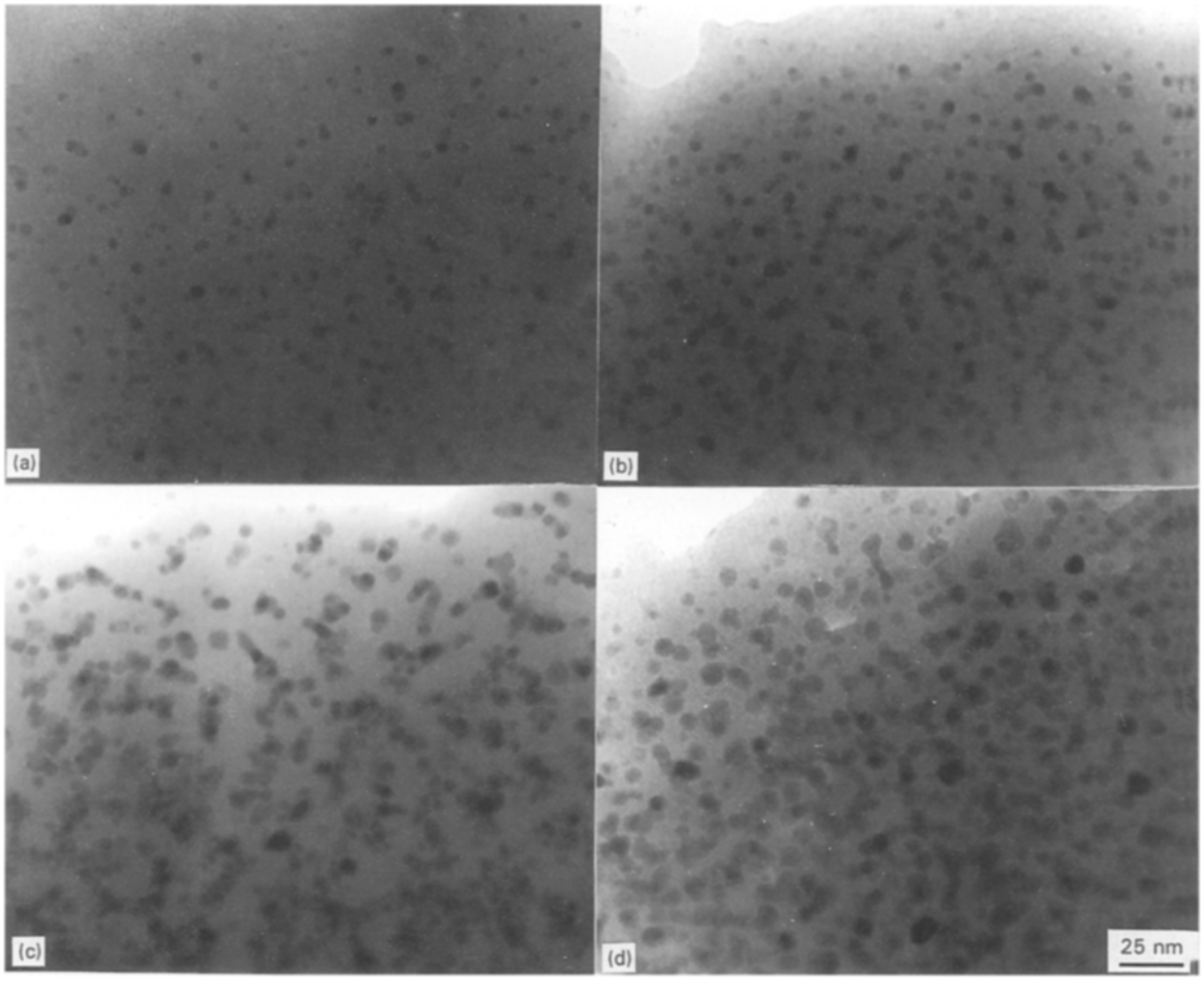

Figure 3 TEM micrographs of the glass samples A, B, C and D.

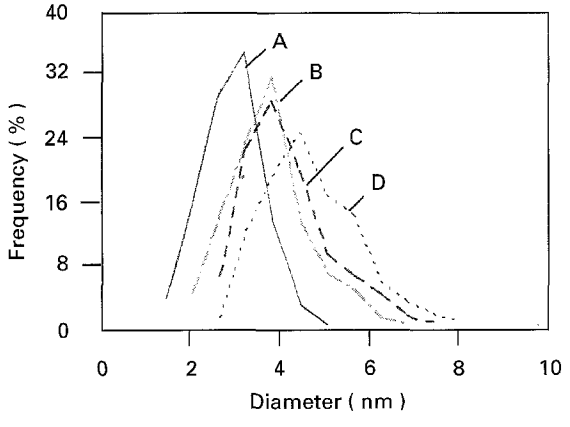

Figure 4 Size distribution of CdS microcrystallites in the glass samples A, B, C and D.

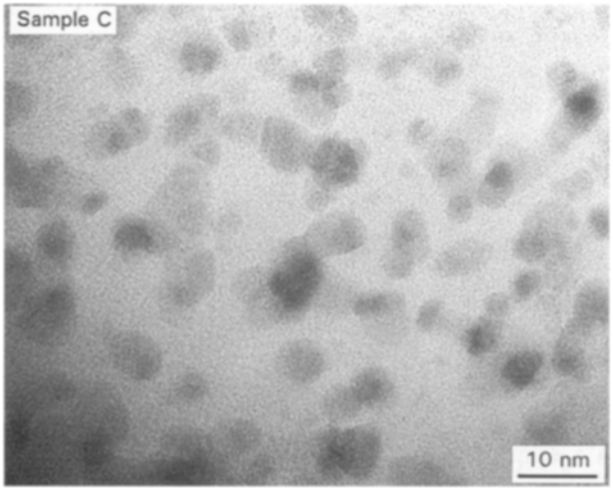

Figure 5 High resolution transmission electron micrograph of CdS microcrystallites dispersed in Na_2O–B_2O_3–SiO_2 glass matrix.

microcrystallites, more measurements and monosized samples are required to elucidate the relationship between $\chi^{(3)}$ and the particle size.

Quantum dots grown by the sol–gel process show drastically different characteristics in the photo-induced absorption behaviour. Fig. 8(a) and (b) show the differential absorption spectra of (a) the sample obtained by melt-quenching technique [25], and (b) the sol–gel derived samples (sample C in particular), respectively. Solid and dashed curves are associated with the $\Delta\alpha L$ spectra taken by subtraction of the unpumped spectrum from the pumped spectrum. The sharp peak at 451 nm in (a) is due to scattering of the pump beam by the sample. The dominant characteristic in Fig. 8(a) and 8(b) is the decrease

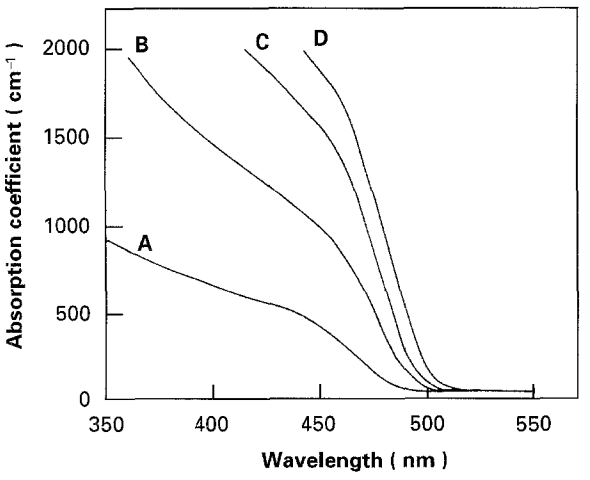

Figure 6 Room temperature absorption spectra of CdS doped glass samples near the resonance wavelength.

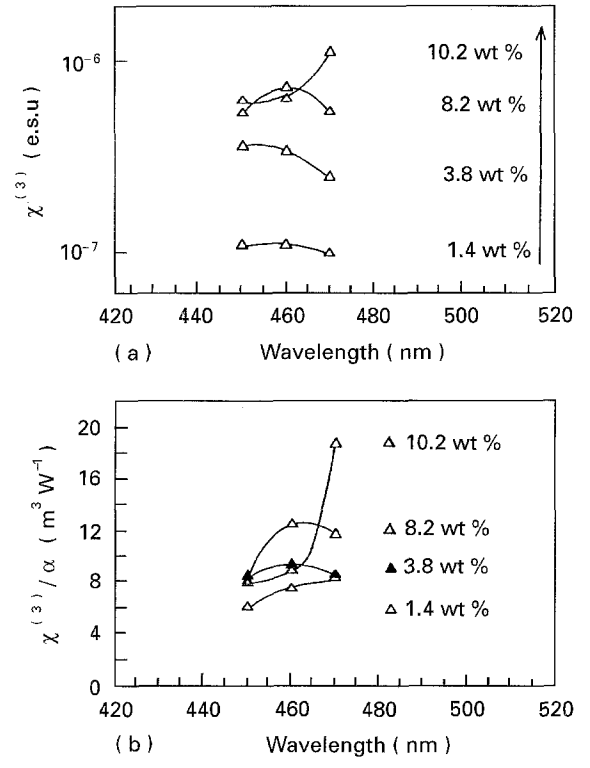

Figure 7 Third-order susceptibilities, $\chi^{(3)}$, of the CdS-doped glass samples measured by DFWM with (a) 7 ns laser pulse and (b) the corresponding $|\chi^{(3)}|/\alpha$ profiles.

in the absorption (negative $\Delta\alpha L$ peak) resulting from bleaching of the exciton state. Very little change is observed in the non-linear spectrum after extensive exposure (2 h) to a pump laser with 5 μJ energy tuned at 451 nm for sample C. This is in direct contrast to the non-linear spectrum obtained from the sample made by the melt-quenching technique [see Fig. 8 (a)] which shows a reduction of $\Delta\alpha L$ by a factor of ≈ 20 as a result of photodarkening after similar pump exposure conditions. The difference in the photodarkening behaviour of the samples may be attributed to the difference in the media surrounding the quantum dots (the difference of the surface ions), and the crystallinity of the quantum dots [6, 23, 26, 27].

The optical non-linearities of semiconductor quantum dots depend on the number of generated carriers.

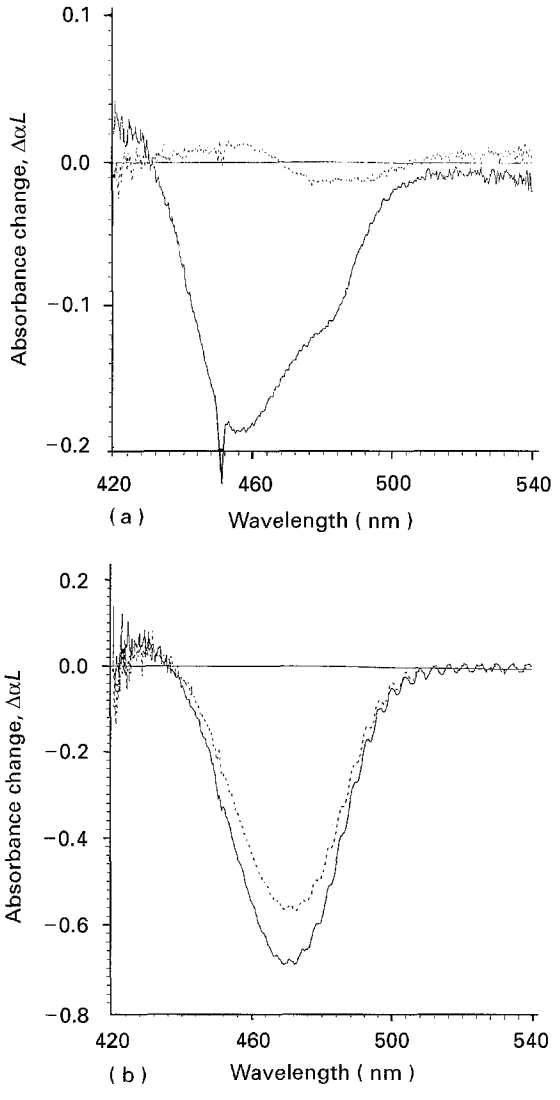

Figure 8 Differential absorption spectra of (a) melt-quenched, and (b) sol–gel derived CdS doped glass sample. Solid and dashed curves are associated with $\Delta\alpha L$ spectra taken before and after extended (2 h) laser exposure, respectively. Pump pulse 5 μJ, 5 ns.

The number of carriers are generally a function of pump intensity, and absorption cross-section of the materials. For normalization of the data, the values of actual change of absorption coefficient $\Delta\alpha$ and refractive index Δn were normalized by the absorption coefficient α at the pumping wavelength. The nonlinear susceptibility, $\chi^{(3)}$, of 10^{-7}–10^{-6} e.s.u. was calculated using the following relationships

$$\Delta n(E) = \frac{ch}{2\pi^2} P \int_0^\infty \frac{\Delta\alpha(E')}{E'^2 - E^2} \mathrm{d}E' \tag{1}$$

$$\Delta\alpha = \frac{4\pi\omega}{nc} Im(\Delta\chi) \tag{2}$$

$$\Delta n = \frac{2\pi}{n} Re(\Delta\chi) \tag{3}$$

Where $n(E)$ is the index of refraction and $\alpha(E)$ is the absorption coefficient, P is the electric susceptibility, $Im(\Delta\chi)$ and $Re(\Delta\chi)$ represent the imaginary and real component of $\Delta\chi$, respectively, E is the electron field of the pump beam, n, c, ω and h are the linear index of diffraction, the velocity of light, incident frequency,

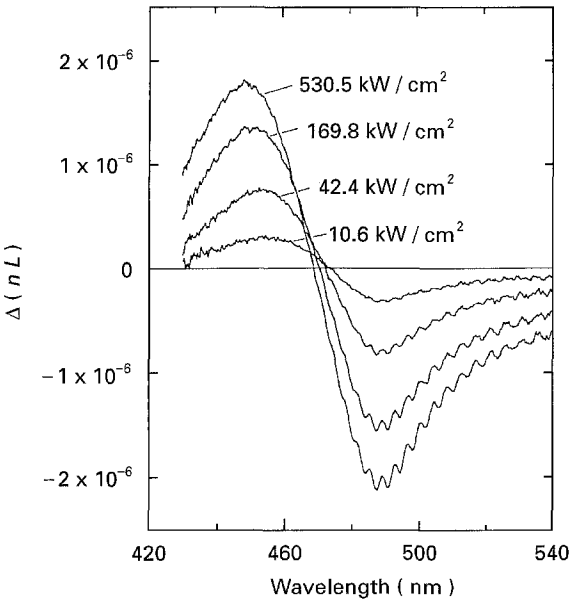

Figure 9 Representative transient index change profiles of CdS quantum dots (sample C) versus pump intensities.

and Planck's constant, respectively. A typical Δn profile versus wavelength for various pump intensities for these samples (sample C in particular) is shown in Fig. 9. The values of Δn were of the order of 10^{-3}–10^{-2} depending on the pump intensity and the concentration of CdS microcrystallites. For factoring out the contribution of pump intensity, $\chi^{(3)}$ was estimated from the values of asymptotic value at the lowest intensity, i.e. the y intercept of the plot of $\Delta\chi/I$ versus I in the range of 5 to 530 kW cm^{-2}.

The subpicosecond time-resolved DFWM experiments were conducted off-resonance and the signals exhibited intensities and decay times that varied with the concentration and particle size of CdS microcrystallites. Results of DFWM measurements with 400 fs laser pulse at 580 nm for sample D are shown in Fig. 10. Similar curves were obtained for the other samples. The data of the xyyx polarization configuration corresponds to an experimental geometry with two excitation pulses (pump) having perpendicular polarization. The signal recorded exhibits the profile of the laser pulses and results from the purely electronic contribution to $\chi^{(3)}$. The yxyx configuration has excitation pulses polarized in parallel, thus the signals here are most probably the result of absorption gratings. It is clear that $\chi^{(3)}_{xxxx}$ is the sum of $\chi^{(3)}_{xyyx}$ and $\chi^{(3)}_{yxyx}$. A good explanation of this polarization dependence can be found in references [3, 28]. Obviously, the fast and slow decay components indicate that there are two distinct excited species, for example bulk and surface states. The signal maximum does not occur at $t = 0$ indicating that there is an inertial relaxation somewhere in the excited state.

The response/decay profile is essentially resolution limited and reveals at least a biexponential decay: a fast non-linear response of 0.5–2.5 ps, and a slow non-linear response of 5–50 ps as a function of the particle size. Fig. 11 shows the relationships between the fast and slow delay times as a function of the

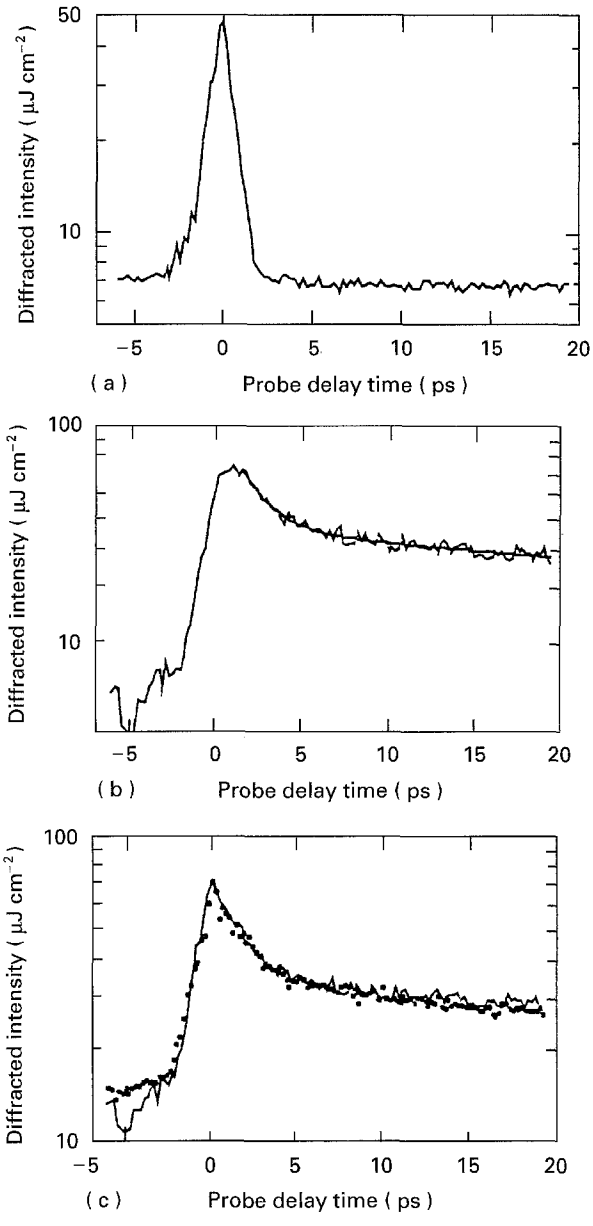

Figure 10 Time response of CdS microcrystallites (sample D) under different polarization configurations of the excitation beams (400 fs at 580 nm, 13 mJ cm^{-2}). (a) xyyx; (b) yxyx; (c) ● data xxxx, — xyyx + yxyx.

average diameter of CdS crystallites (a) and their concentration (b). It is clear that both the fast and slow delay times increase as the size and/or concentration of CdS microcrystallites increases. This can be explained by the lattice heating of CdS crystallites which cools by diffusion to the host. Since the local-field is constant, each particle absorbs the same amount of energy per unit volume. The volume is proportional to r^3, but the surface area is proportional to r^2, resulting in a thermal buildup for the larger particles [29]. Clearly, more research is required if we are to achieve an understanding of the non-linear-optical properties of these materials.

Finally, a self-diffraction experiment using 400 fs laser-induced grating was performed at room temperature. Self-diffraction arising from the interaction between two input laser beams was observed in all the samples. Fig. 12 shows the diffraction fluence at various diffraction orders for sample D. The non-linearities contributing to the laser-induced grating are of

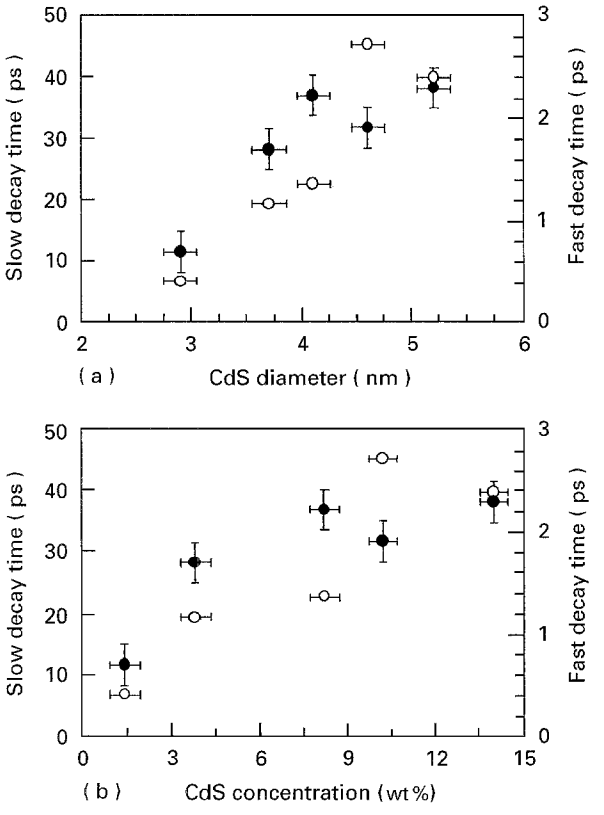

Figure 11 Change of the fast (●) and slow (○) decay time as a function of (a) the particle size, and (b) CdS concentration of CdS quantum dots in the glasses.

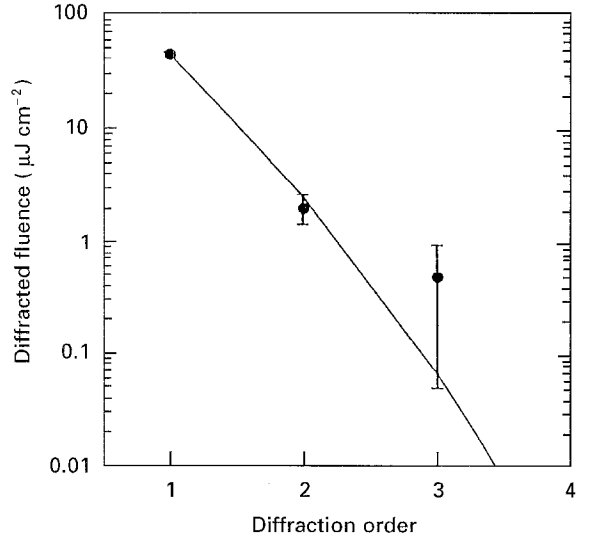

Figure 12 Self-diffraction results for sample D by the 400 fs laser pulse. Fluence = 13 mJ cm^{-2}.

coherent and incoherent (e.g. bleaching) nature. To express both contributions together by $\chi^{(3)}_{eff}$, a $\chi^{(3)}$ value of 10^{-12}–10^{-11} e.s.u. was calculated based on Fig. 12 under off-resonance condition, at 580 nm [18].

4. Conclusions

CdS quantum dots of high crystallinity and diameter of 3–6 nm, embedded in Na_2O–B_2O_3–SiO_2 glasses, have been prepared by the sol–gel process. Resonant $\chi^{(3)}$ values as high as 10^{-6} e.s.u. for these quantum dots has been determined by both DFWM and pump-probe measurements using 5–7 ns laser pulse at wavelengths of 450–470 nm at room temperature. The off-resonance $\chi^{(3)}$ for these samples was determined to be on the order of 10^{-12}–10^{-11} e.s.u. for laser pulse with subpicosecond duration (400 fs) at wavelength 580 nm by the time-resolved DFWM experiments (self-diffraction). It was found that the $\chi^{(3)}$ value of these samples was linearly proportional to the concentration of CdS microcrystallites in the glasses. Biexponential decays of 0.5–2.5 ps (fast) and 5–50 ps (slow) were observed under 400 fs laser pulse excitation, which are also linearly proportional to the concentration and particle size of CdS microcrystallites in the glasses.

The results reported in this paper can be further improved by controlling the particle size and size distribution of CdS microcrystallites. Recently we have developed a novel process to prepare samples with monosized particles [30]. However, the present achievements are important and promising for all-optical device applications. The glasses that have been produced are close to the threshold value for $|\chi^{(3)}|/\alpha$ which would allow manufacture of workable practical devices [12]

Acknowledgements

The authors are grateful to the Air Force Office of Scientific Research, Directorate of Chemical and Materials Science, AFOSR, and Strategic Defense Initiative Organization for the financial support of this work. We would also like to thank Dr Jie Zhang and Professor Leroy Eyring of the Center for Solid State Science, Arizona State University for the high resolution transmission electron microscopy work.

References

1. N. PEYGHAMBARIAN, S. W. KOCH, H. M. GIBBS and H. HAUG, in "Nonlinear optics and optical computing" edited by S. Martellucci and A. N. Chester (Plenum Press, New York, 1990).
2. R. W. BRYANT, "Nonlinear optical materials; New Technologies, Applications, Markets" (Business Communications Co., Inc., Norwalk, 1989).
3. R. K. JAIN and R. C. LIND, *J. Opt. Soc. Amer.* **73** (1983) 647.
4. J. YUMOTO, S. FUKUSHIMA and K. KUBOTERA, *Opt. Lett.* **12** (1987) 832.
5. P. ROUSSIGNOL, D. RICARD, J. LIKASIK and C. FLYTANIS, *J. Opt. Soc. Amer. B* **4** (1987) 5.
6. T. YANAGAWA, H. NAKANO, Y. ISHIDA and Y. SASAKI, *Opt. Commun.* **88** (1992) 371.
7. B. VAN WONTERGHEM, S. M. SALTIEL, T. E. DUTTON and P. M. RENTZEPIS, *J. Appl. Phys.* **66** (1989) 4935.
8. K. W. DELONG, A. GABEL, C. T. SEATON and G. I. STEGEMAN, *J. Opt. Soc. Amer. B* **6** (1989) 1306.
9. E. M. WRIGHT, S. W. KOCH, J. E. EHRLICH, C. T. SEATON and G. I. STEGEMAN, *Appl. Phys. Lett.* **52** (1988) 2128.
10. T. TAKADA, T. YANO, A. YASUMORI, M. YAMANE and J. D. MACKENZIE, *J. Non-Cryst. Solids* **147 & 148** (1992) 631.
11. M. YAMANE, T. TAKADA, J. D. MACKENZIE and C-Y. LI, *SPIE Proc.* **1758** "Sol–gel optics II" San Diego, July, 1992.
12. C. LI, Y. KAO, K. HAYADHI, T. TAKADA and J. D. MACKENZIE, *SPIE Proc.* **2288** "Sol–gel optics III" San Diego, July, 1994.

13. N. F. BORRELLI, D. W. HALL, H. J. HOLLAND and D. W. SMITH, *J. Appl. Phys.* **61** (1987) 5399.
14. H. HIRAGA, S. OMI, K. UCHIDA, C. HARA, Y. ASAHARA, A. IKUSHIMA, T. TOMOZAKI and A. NAKAMURA, in Proceedings of 2nd Meeting on Glasses for Optoelectronics, Tokyo, January 18, 1991.
15. Y. Z. HU, S. W. KOCH, M. LINDBERG, N. PEYGHAMBARIAN, E. L. POLLOCK and FARID F. ABRAHAM, *Phys. Rev. Lett.* **64** (1990) 1805.
16. S. H. PARK, R. A. MORGAN, Y. Z. HU, M. LINDBERG, S. W. KOCH and N. PEYGHAMBARIAN, *J. Opt. Soc. Amer. B* **7** (1990) 2097.
17. T. TOKIZAKI, H. AKIYAMA, M. TAKAYA and A. NAKAMURA, *J. Cryst. Growth* **117** (1992) 603.
18. R. J. REEVES, R. C. POWELL, E. T. KNOBBE, C. LI, J. D. MACKENZIE, T. TAKADA and M. YAMANE, in Proceedings of 1992 OSA Annual Meeting, Albuquerque, New Mexico Sept. 1992.
19. D. RECARD, P. ROSSIGNOL, F. HACH and CH. FLYTZANIS, *Phys. State. Sol. (b)* **159** (1990) 275.
20. M. G. BAWENDI, W. L. WILSON, L. ROTHBERG, P.L. CARROLL, T. M. JEDJU, M. L. STEIGERWALD and L. E. BRUS, *Phys. Rev. Lett.* **65** (1990) 1623.
21. A. I., AL. L. EFROS and A. A. ONUSHCHENKO, *Solid State Commun.* **56** (1985) 921.
22. L. BRUS, *J. Phys. Chem.* **90** (1986) 2555.
23. B. G. POTTER, JR. and J. H. SIMMONS, *Phys. Rev. B* **37** (1988) 10838.
24. F. HACHE, D. RICARD and C. FLYTZANIS, *J. Opt. Soc. Amer. B* **3** (1986) 1647.
25. L-C. LIU and S. H. RISBUD, *J. Appl. Phys.* **68** (1990) 28.
26. K. KANG, A. D. KEPNER, Y. Z. HU, S. W. KOCH, N. PEYGHAMBARIAN, C.-Y. LI, T. TAKADA, Y. KAO and J. D. MACKENZIE, *Appl. Phys. Lett.* **64** (1994) 1487.
27. D. W. HALL and N. F. BORRELLI, *J. Opt. Soc. Amer. B* **5** (1988) 1650.
28. F. HACHE, D. RICARD, C. FLYTZANIS and U. KREIBIG, *Appl. Phys. A* **47** (1988) 347.
29. M. J. BLOEMER, J. W. HAUS and P. R. ASHLEY, *J. Opt. Soc. Amer. B* **7** (1990) 790.
30. T. TAKADA, J. TSENG, C.-Y. LI, J. M. MACKENZIE and M. YAMANE, *J. Sol–gel Sci. Technol* **1** (1994) 123.

Received 2 September 1994
and accepted 22 March 1995